Ferromagnetic nanostructures of oxygen on Ag(111)

Ferromagnetic nanostructures of oxygen on Ag(111)

Y Kunisada, H Nakanishi, W A Diño and H Kasai

Department of Applied Physics, Osaka University,
2-1 Yamada-oka, Suita, Osaka 565-0871, Japan

Email: kasai@dyn.ap.eng.osaka-u.ac.jp

Abstract. First principles calculations were performed to investigate the robustness of oxygen adsorbed structures that show ferromagnetic properties. These ferromagnetic properties are induced by ferromagnetic superexchange interactions and Ruderman-Kittel-Kasuya-Yosida (RKKY) interactions. Such ferromagnetic oxygen adsorbed structures appear only in the case of coverages higher than 0.5 ML, because the ferromagnetic superexchange interactions and RKKY interactions are appreciable between O-O only for short distances. In this work, we focused on single oxygen atom diffusion parallel and perpendicular to Ag(111) surfaces. The in-plane diffusion could induce associative desorption, which reduces the oxygen coverage. On the other hand, diffusion to the subsurface could quench the magnetic moment. These diffusion paths have effective diffusion barriers of 0.78 eV. Thus, such diffusion rarely occurs in low temperature regions.

1. Introduction

Surface magnetism has attracted a great deal of interest in basic science and application fields. From the viewpoint of basic science, singular behaviours of magnetic impurities [1-8] (and references therein) on surfaces have been investigated, and are caused by the two-dimensionality of the surface. In addition, understanding and controlling these singular behaviours are also very important for realizing high capacitance and robustness of magnetic devices. Moreover, studies suggested that surface magnetic states can be useful for controlling catalytic reactivity [9-13] in fuel cell electrodes. These studies show that the efficacy of surface magnetism extends from spintronics devices to energy-related technologies. Design and control of magnetic surfaces are promising ways for developing new effective devices and catalysts.

Recently, we reported metastable ferromagnetic states of the O/Ag(111) system [14,15] by potential energy surface (PES) studies on O_2 dissociative adsorption on Ag(111) surfaces, and suggested possibilities for controlling the surface magnetic properties in this system. The ferromagnetic oxygen adsorbed structures on Ag(111) surfaces are induced by the ferromagnetic superexchange interactions and Ruderman-Kittel-Kasuya-Yosida (RKKY) interactions. Such ferromagnetic oxygen adsorbed structures appear only in the case of coverages higher than 0.5 ML, because the ferromagnetic superexchange interactions and RKKY interactions are appreciable between O-O only for short distances. In this work, we investigated the robustness of ferromagnetic oxygen adsorbed structures on Ag(111) surfaces. Especially, we focused on oxygen atom diffusion parallel and perpendicular to Ag(111) surfaces in the case of 0.5 ML coverage. In-plane oxygen atom diffusion, which corresponds to oxygen atom motion parallel to Ag(111) surfaces, makes the distance between oxygen atoms shorter, which changes the stable oxygen adsorbed structures to unstable ones. Oxygen atom diffusion into the subsurface, which correspond to oxygen atom motion perpendicular to Ag(111) surfaces,

contributes to quenching the ferromagnetic states. Thus, we performed first principles investigations of oxygen atom diffusion by calculating the relevant potential energy curves. From these potential energy curves, we could obtain the diffusion barrier heights and diffusion coefficients.

2. Computational methods

We performed spin-polarized total energy calculations based on density functional theory (DFT), using the generalized gradient approximation (GGA) within the Perdew-Burke-Ernzerhof (PBE) functional for the exchange–correlation energy [16,17], which is implemented using the plane-wave and projector augmented wave method [18-21]. We applied a 600 eV cutoff to limit the plane-wave basis set without compromising computational accuracy. A 5x5x1 Monkhorst–Pack special k-point grid [22] for Brillouin zone sampling using a Gaussian smearing model of σ=0.05 eV was used. First, for the O/Ag(111) system, the Ag substrate was simulated by a slab of four fcc (2x2) Ag(111) layers. The supercell was constructed with a 1.55 nm vacuum separation between slabs. Lateral and interlayer Ag–Ag distances for this system are initially set based on the theoretically predicted equilibrium lattice constant of 0.294 nm, obtained by using a 9x9x9 k-mesh on a primitive one-atom fcc unit cell for bulk Ag. In order to determine the optimized Ag(111) surface structure, we performed calculations in which the top two layers are relaxed. The total energy convergence with this size of supercell is within 10 meV. Hence, the above parameters gave acceptable accuracy. Moreover, the magnetic moment converges to 0.01 μ_B. Because the mass of an oxygen atom is much lighter than that of an Ag atom, we expect a large difference in the time scales associated with surface relaxations and oxygen atom dynamics. Thus, as a first step, we neglected surface relaxations. In these calculations, we adopted an electric dipole correction layer in the vacuum area to compensate for the dipole interactions between the repeated slabs [23]. Lastly, electron transfer is obtained from the difference between the electron density distribution of two configurations of oxygen: isolated from and adsorbed on the substrate, using Bader charge analysis [24,25].

In Figure 1, we show 0.5 ML oxygen adsorbed structures on Ag(111) surfaces, which show ferromagnetic behaviours. In this work, we call these configurations (a) f-f and (b) h-f configurations. Two oxygen atoms in the supercell are above fcc hollow sites in the f-f configuration, and one oxygen atom is above a hcp hollow site and the other is above a fcc hollow site in the h-f configuration. In the f-f and h-f configurations, the magnetic moments of oxygen atoms remain as 0.32 μ_B and 0.49 μ_B, respectively. Also, in these configurations, the magnetic moment of the nearest Ag atom is 0.09 μ_B. For reference, we mention that the h-h configuration, which has two oxygen atoms in the supercell above hcp hollow sites, has almost the same magnetic properties as the f-f configuration. Such ferromagnetic oxygen adsorbed structures appear only for higher coverage than 0.5 ML, because the ferromagnetic superexchange interactions and RKKY interactions are appreciable between O-O only for short distances. We also estimated the Curie temperature using mean field theory. The corresponding Curie temperature is 305 K. Our previous PES studies [14,15] show that the f-f, h-h, an h-f configurations have corresponding activation barriers for O_2 dissociative adsorptions of 1.37, 1.43, and 2.17 eV, and potential energies with metastable dissociative adsorption states of 0.355, 0.543, 0.552 eV, respectively, where the sum of the energies of the Ag slab and of the isolated O_2 is chosen as the origin of the potential energy. Thus, the metastable dissociative adsorption states that we have observed have associative desorption barrier heights of 0.9~1.6 eV, which were calculated from differences between the corresponding activation barriers and the potential energies with metastable dissociative adsorption states. As expected, these desorption barriers are smaller than that for a lower coverage case (0.40 ML), whose desorption barriers are 2.68±0.17 eV based on experimental results [26]. The uptake coverage of dissociative oxygen adsorption at a surface temperature of 160 K is 0.40 ML. Thus, we can deduce that a surface temperature lower than 160 K is required to realize these 0.5 ML coverages. Nevertheless, the high coverage structures are still stable. In this work, we chose the f-f configuration as the initial structure before oxygen atom diffusion, because the f-f configuration is the most stable at a 0.5 ML coverage.

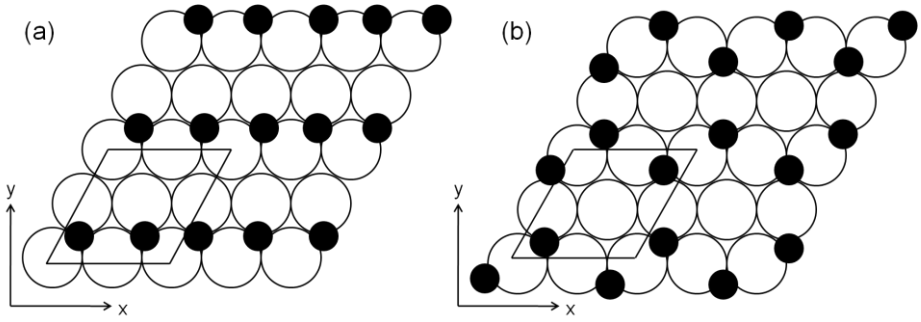

Figure 1. Oxygen adsorbed structures with (a) f-f and (b) h-f configurations. Two oxygen atoms in the supercell are above fcc hollow sites in the f-f configuration, and one oxygen atom is above a hcp hollow site and the other is above a fcc hollow site in the h-f configuration. Black and white circles show the positions of O and Ag atoms, respectively, and the parallelogram shows the supercell of fcc (2x2) Ag(111) surfaces.

3. Results and discussion

We investigated in-plane oxygen atom diffusion on Ag(111) surfaces in the case of 0.5 ML coverage. We considered that one oxygen atom moves to a hcp hollow site in the f-f configuration. In Figure 2, we show the three diffusion paths that we considered. The fixed oxygen atom (A) in Figure 2 is 0.12 nm above the first Ag(111) layer.

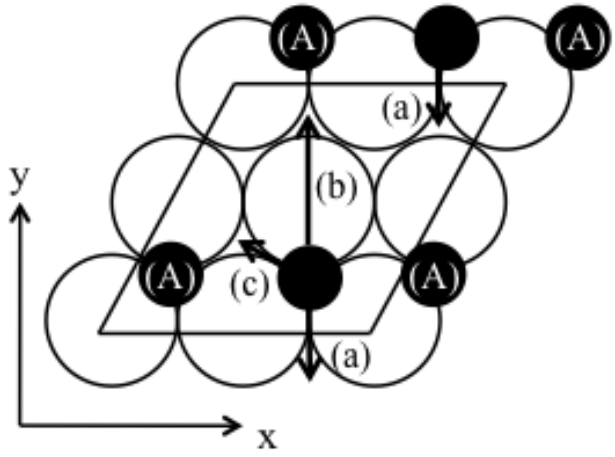

Figure 2. The three diffusion paths that we considered. Black and white circles show the positions of O and Ag atoms, respectively, and the parallelogram shows the supercell of fcc (2x2) Ag(111) surfaces. The position of oxygen atom (A) is fixed.

In Figure 3, we show potential energy curves for each diffusion path. The potential energy values are checked at 0.02 nm and 0.04 nm intervals for directions perpendicular and parallel to the Ag(111) surface, respectively. These intervals are sufficiently small so that the accuracy of the calculated potential energy curves is ensured. Here, we set the energy origin to correspond to the most stable f-f configuration. The paths along (a), (b), and (c) have diffusion barrier heights of 0.33, 1.22, and 0.80 eV, respectively. In the case of 0.11 ML coverage, which consists of one oxygen atom and fcc (3x3) Ag(111) layers, oxygen atom diffusion from a fcc hollow site to a hcp hollow site over bridge and top sites has a diffusion barrier height of 0.41 and 1.40 eV, respectively. It should be noted that the diffusion barrier heights are reduced in paths (a) and (b) and increased in path (c) because of repulsion between oxygen atoms. The diffusion along path (a) does not contribute to oxygen desorption, because this diffusion results only in a change between the f-f and h-f configurations. On the other hand,

diffusion along paths (b) and (c) makes the distance between the two oxygen atoms shorter. After such diffusion, the two oxygen atoms can become desorbed as an oxygen molecule with no desorption barrier [14]. From these calculations, we found that diffusion along paths (b) and (c) prevents the realization of high coverages. We also estimated the zero point energies along these diffusion paths using a harmonic potential approximation of each potential well. These zero point energies are about 20 meV. In comparison with the diffusion barrier heights, the zero point energies do not make a significant contribution to the diffusion. Finally, we can say that the effective in-plane diffusion barrier height for breaking ferromagnetic oxygen adsorbed structures is about 0.78 eV. This value is almost the same order as the associative desorption barrier height. We also calculated the diffusion coefficient for oxygen atom diffusion Γ using the Arrhenius equation

$$\Gamma = \Gamma_0 \exp\left(-\frac{E}{k_B T}\right), \quad (1)$$

where Γ_0, E, k_B, and T are the diffusion prefactor, the effective diffusion barrier height, the Boltzmann constant, and the temperature of the system, respectively. Estimating the diffusion prefactor from the attempt frequency, which is approximately the same as the oxygen atom vibration frequency, the diffusion coefficients for in-plane diffusion are 3.5×10^{-10} nm^2/s at 160 K and 98 nm^2/s at 300 K.

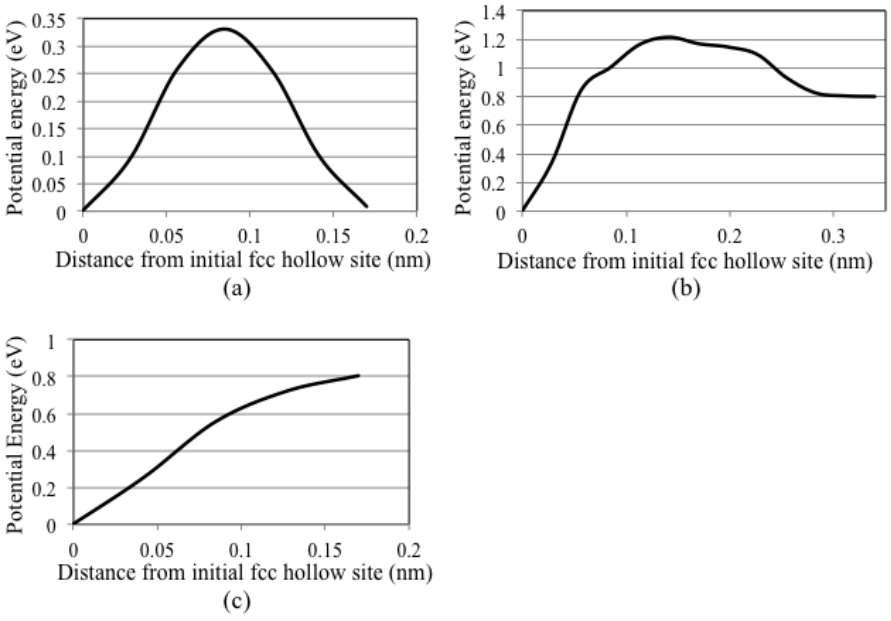

Figure 3. Potential energy curves for diffusion paths (a), (b), and (c), as indicated in Figure 2. The energy origin was set to the most stable f-f configuration.

We also focused on the penetration of one oxygen atom through the surface Ag layer from an on-surface fcc hollow site to a subsurface site in the f-f configuration. The fixed oxygen atom is 0.12 nm from the first Ag(111) layer. In Figure 4, we show the potential energy curve for oxygen atom diffusion to the subsurface. The step size perpendicular to the Ag(111) surfaces is 0.02 nm, which is sufficiently small so that the accuracy of the calculated potential energy curve is ensured. Here, we set the energy origin to the most stable f-f configuration. The diffusion barrier height for the penetration is 5.54 eV. We also performed a calculation in which the top two layers are relaxed with oxygen atoms in the topmost Ag layer. Then, the corresponding diffusion barrier height is reduced to 0.79 eV. This value is almost the same as the 0.81 eV diffusion barrier height obtained in the case of 0.11 ML coverage [27]. We also estimated the zero point energy along the diffusion path using the harmonic potential approximation. The zero point energy is about 10 meV. Thus, the effective diffusion barrier height is 0.78 eV. After the penetration, oxygen atoms gain more electrons from the Ag(111) surfaces

and magnetic moments are quenched. Hence, this diffusion contributes to quenching the ferromagnetic states. It should also be noted that the corresponding diffusion coefficients for diffusion into the subsurface are 2.2×10^{-10} nm^2/s at 160 K and 62 nm^2/s at 300 K.

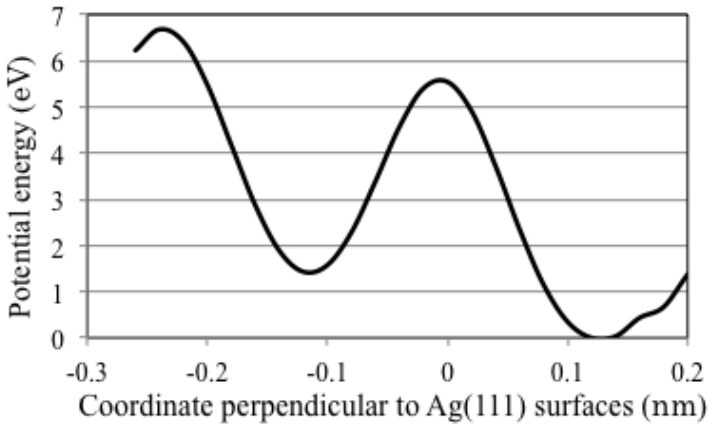

Figure 4. Potential energy curve of diffusion perpendicular to Ag(111) surfaces. The origin of the coordinates perpendicular to Ag(111) surfaces was set to the topmost Ag(111) layer. The energy origin was set to the most stable f-f configuration.

4. Summary

We performed first principles investigations on the robustness of ferromagnetic oxygen adsorbed structures on Ag(111) surfaces. We focused on oxygen atom diffusion parallel and perpendicular to Ag(111) surfaces. The in-plane diffusion can make O-O distances shorter and induce associative desorption, which reduces the oxygen coverage. On the other hand, diffusion of oxygen atoms into the subsurface can quench the magnetic moment. Consequently, such diffusion must be suppressed to realize and maintain the ferromagnetic oxygen adsorbed structures. These diffusion paths have an effective diffusion barrier of 0.78 eV. We also calculated the diffusion coefficients for oxygen atom diffusion using an Arrhenius equation. The diffusion coefficients for in-plane diffusion are 3.5×10^{-10} nm^2/s at 160 K and 98 nm^2/s at 300 K. The diffusion coefficients for diffusion into the subsurface are 2.2×10^{-10} nm^2/s at 160 K and 62 nm^2/s at 300 K. Thus, once ferromagnetic oxygen adsorbed structures form, diffusion rarely occurs in the experimentally-used low temperature region below 160 K, which is considered to be required for 0.5 ML coverage. From the results of a hyperthermal O_2 molecular beam experiment involving oxidation of Cu(111) surfaces [28], it has been reported that the oxidation process strongly depends on the O_2 translational energy, surface temperature and surface diffusion. We must optimize these parameters to realize coverages higher than 0.4 ML. Hence, we must consider these dynamics effects in the oxidation process to realize high coverages. These oxidation dynamics are ongoing studies.

Acknowledgments

This work is supported by MEXT (Ministry of Education, Culture, Sports, Science and Technology) through the G-COE (Special Coordination Funds for the Global Center of Excellence) program (H08) "Atomically Controlled Fabrication Technology", Grant-in-Aid for Scientific Research on Innovative Areas Program (2203-22104008) and Scientific Research (A) 20246011, (c) 22510107 program; by JST (Japan Science and Technology Agency) through ALCA (Advanced Low Carbon Technology Research and Development) Program " Development of Novel Metal-Air Secondary Battery Based on Fast Oxide Ion Conductor Nano Thickness Film" and Elements Science and Technology Project "New development of self-forming nano-particle catalyst without precious metals". Calculations were done using computer facilities of the Cyber Media Center (Osaka University) and the ISSP Super Computer

Center (the University of Tokyo). YK would like to extend gratitude to the Japan Society for Promotion of Science (JSPS) Young Researcher Fellowship for funding.

References

[1] Fisher B F and Klein M W 1975 *Phys. Rev. B* **11** 2025
[2] Silly F, Pivetta M, Ternes M, Patthey F, Pelz J P, and Schneider W D 2004 *Phys. Rev. Lett.* **92** 016101
[3] Negulyaev N N, Stepanyuk V S, Niebergall L, Bruno P, Pivetta M, Ternes M, Patthey F and Schneider W D 2004 *Phys. Rev. Lett.* **102** 246102
[4] Hoa N T M, Minamitani E, Diño W A, Cong B T and Kasai H 2010 *J. Phys. Soc. Jpn.* **79** 074702
[5] Minamitani E, Diño W A, Nakanishi H and Kasai H 2010 *Surf. Sci.* **604** 2139
[6] Minamitani E, Diño W A, Nakanishi H and Kasai H 2010 *Phys. Rev. B* **82** 153203
[7] Hoa N T M, Diño W A and Kasai H 2010 *J. Phys. Soc. Jpn.* **79** 113706
[8] Hoa N T M, Diño W A and Kasai H *J. Phys. Soc. Jpn.* accepted
[9] Escaño M C, Nguyen T Q, Nakanishi H and Kasai H 2009 *J. Phys.: Condens. Matt.* **21** 49221
[10] Escaño M C, Nakanishi H and Kasai H 2009 *J. Phys. Chem.* **113** 14302
[11] Tsuda M, Diño W A, Watanabe S, Nakanishi H and Kasai H 2004 *J. Phys. Condens. Matter* **16** S5721
[12] Tsuda M, Diño W A, Watanabe S, Nakanishi H and Kasai H 2004 *e-J. Surf. Sci. Nanotech.* **2** 200
[13] Zeng J, Liao S, Lee J Y, Liang Z 2010 *Int'l. Journal of Hydrogen Energy* **35** 942
[14] Kunisada Y, Nakanishi H and H. Kasai 2011 *J. Phys. Soc. Jpn.* **80** 084605
[15] Kunisada Y, Escaño M C and H. Kasai 2011 *J. Phys.: Condens. Matt.* **23** 394207
[16] Perdew J P, Burke K and Ernzerhof M 1996 Phys. Rev. Lett. **77** 3865
[17] Perdew J P, Burke K and Ernzerhof M 1997 Phys. Rev. Lett. **78** 1396
[18] Kresse G and Furthmüller J 1996 Comput. Mater. Sci. **6** 15
[19] Kresse G and Furthmüller J 1996 Phys. Rev. B **54** 11169
[20] Kresse G and Hafner J 1993 Phys. Rev. B **47** 558
[21] Kresse G and Hafner J 1994 Phys. Rev. B **49** 14251
[22] Monkhorst H J and Pack J D 1976 Phys. Rev. B **13** 5188a
[23] Neugebauer J and Scheffler M 1992 Phys. Rev. B **46** 16067
[24] Bader R F W 1990 Atoms in Molecules: A Quantum Theory (Oxford: Oxford University Press)
[25] Henkelman G, Arnaldsson A and Jonsson H 2006 Comput. Mater. Sci. **36** 354
[26] Raukema A, Butler D A, Box F M A and Kleyn A W1995 Surf. Sci. **347** 151
[27] Li W X, Stampfl C and Scheffler M 2003 Phys. Rev. B **67** 045408
[28] Moritani K, Okada M, Sato S, Goto S, Kasai T, Yoshigoe A and Teraoka Y 2004 J. Vac. Sci. Technol. A **22** 1625